Atmos. Chem. Phys. Discuss., 12, 12759–12800, 2012
www.atmos-chem-phys-discuss.net/12/12759/2012/
doi:10.5194/acpd-12-12759-2012

Atmospheric Chemistry and Physics Discussions

Evaluation of atmosphere-biosphere exchange estimations with TCCON measurements

J. Messerschmidt[1], N. Parazoo[2], N. M. Deutscher[3], C. Roehl[1], T. Warneke[3], P. O. Wennberg[1], and D. Wunch[1]

[1]California Institute of Technology, Pasadena, CA, USA
[2]Jet Propulsion Laboratory, Pasadena, CA, USA
[3]Institute of Environmental Physics, Bremen, Germany

Received: 30 April 2012 – Accepted: 4 May 2012 – Published: 22 May 2012

Correspondence to: J. Messerschmidt (janina@caltech.edu)

Published by Copernicus Publications on behalf of the European Geosciences Union.

Abstract

Three estimates of the atmosphere-biosphere exchange are evaluated using Total Carbon Column Observing Network (TCCON) measurements. We investigate the Carnegie-Ames-Stanford Approach (CASA), the Simple Biosphere (SiB) and the GBiome-BGC models transported by the GEOS-Chem model to simulate atmospheric CO_2 concentrations for the time period between 2006 and 2010. The CO_2 simulations are highly dependent on the choice of the atmosphere-biosphere model and large-scale errors in the estimates are identified through a comparison with TCCON data. Enhancing the CO_2 uptake in the boreal forest by 40 % and shifting the onset of the growing season significantly improve the simulated seasonal CO_2 cycle using CASA estimates. The SiB model gives the best estimate for the atmosphere-biosphere exchange in the comparison with TCCON measurements.

1 Introduction

Understanding, quantifying and predicting the atmospheric carbon cycle is a challenging task, since global transport, carbon fluxes due to fossil fuel emissions, ocean-atmosphere exchange, and biosphere-atmosphere exchange must all be known. Thus, an accurate estimation of carbon fluxes is a central goal of the carbon cycle community. Such estimates have been derived on small spatial scales using direct measures of the fluxes via eddy-covariance (e.g., http://fluxnet.ornl.gov/) and by carbon stock analysis (e.g., Gaudinski et al., 2000; Goodale et al., 2002). On larger spatial scales, inverse or "top down" methods have been attempted using measurements of the spatial and temporal variations in atmospheric CO_2 concentrations. Typically, these inverse studies use "Bayesian" methods where "a priori" estimates are combined with atmospheric observations and an atmospheric transport model. The "a priori" estimates represent the best knowledge of the global flux distribution (e.g., Baker et al., 2006; Peters et al., 2007) or the distribution of flux proxies (Michalak et al., 2004). The resulting a posteriori

Discussion Paper | Discussion Paper | Discussion Paper | Discussion Paper |

ACPD

12, 12759–12800, 2012

flux estimates are the optimal estimates as determined by the assigned error covariance based on the assumed a priori distribution, the observations and the atmospheric transport model.

In inverse methods, unless the design of the inverse machinery is carefully constructed, errors in the a priori distribution at one spatial scale can alias into errors in the inferred distribution at other spatial scales. In particular, developers must make choices about the spatial and temporal scale at which they retrieve fluxes. In theory, such choices are determined by the scales that drive the variance in the observations, but in practice, computational considerations may limit the resolution of the model.

The substantial impact of synoptic scale weather systems (e.g., 3–10 days) in driving local variability in atmospheric CO_2 has been illustrated in recent studies (e.g., Keppel-Aleks et al., 2011; Parazoo et al., 2008). Meridional advection produces significant local variability in atmospheric CO_2 during the Northern Hemisphere summertime, when there are strong north-south gradients in CO_2. Such variance is driven at hemispheric scales, and so the inverse method must extend to global scales. Traditionally, atmospheric inverse modeling has been based on a global network of in situ boundary layer measurement stations. Hence, large-scale errors in the a priori distribution, like an incorrect north-south CO_2 gradient, can alias into errors at local scale around the in situ boundary layer measurement stations in the optimization, generally yielding local/regional flux variability that is too large. Thus, accurate large-scale fluxes are critical for estimating accurate local fluxes, because errors in the description of large-scale flux patterns will alias into the retrieved regional scale fluxes.

Total column measurements are expected to improve the constraint on carbon cycle processes (Rayner and O'Brien, 2001; Yang et al., 2007). These data are particularly helpful for this evaluation because variations in total column measurements are dominated by hemispheric flux distributions, and local and regional fluxes have only a minor impact (Keppel-Aleks et al., 2012). Hence, total column measurements provide a largely independent piece of information to in situ boundary layer measurements, which are mostly driven by local influences.

Keppel-Aleks et al. (2012) estimated the north-south CO_2 gradient using total column measurements from the Total Carbon Column Observing Network (TCCON) by correlating the CO_2 abundances to the potential temperature, which serves as a dynamical tracer for synoptic-scale dynamics. Additionally, the authors showed that the seasonal CO_2 amplitude seen in total column measurements is dominated by the net ecosystem exchange (NEE) in the boreal forest and the temporal phase of the uptake. The CO_2 fields were simulated with a general circulation model (GCM) and the NEE was estimated by the CASA model. In a sensitivity study, the NEE was enhanced by 40 % in the boreal forest and the onset of the growing season was shifted earlier. These changes significantly improved the comparison of the simulation with the total column measurements.

Here, we evaluate three a priori NEE flux distributions using the GEOS-Chem global three-dimensional (3-D) chemical transport model (CTM) driven by year-specific meteorological input data. The net ecosystem exchange (NEE) is defined in this work as follows: a net CO_2 flux from the ecosystem to the atmosphere is positive and referred to as net CO_2 release. A net CO_2 flux from the atmosphere to the ecosystem is negative and referred to as net CO_2 uptake. We analyze the following distinct atmosphere-biosphere exchange inventories: the Carnegie-Ames-Stanford Approach (CASA, Olsen and Randerson, 2004, described in Sect. 3), the Simple Biosphere model (SiB, Baker et al., 2003, described in Sect. 4) and the GBiome-BGC model (Trusilova and Churkina, 2008, described in Sect. 5). The CO_2 total column abundances from these model runs are compared with measured columns from the TCCON (Sect. 7). The GEOS-Chem model and TCCON observations are described in Sect. 2 and 6, respectively. Additionally, we investigate a simulation with CASA, but with uptake enhanced in the boreal forest and with the onset of the growing season shifted according to Keppel-Aleks et al. (2011) (Sect. 7). An improved and year-specific NEE flux inventory for the years 2006–2010 is presented in Sect. 8. GEOS-Chem CO_2 simulations using this inventory are compared with GLOBALVIEW-CO2 data (GLOBALVIEW-CO2, 2011) and total column CO_2 measurements at four Northern Hemisphere TCCON sites (Sect. 8).

ACPD
12, 12759–12800, 2012

2 GEOS-Chem CO_2 simulation

GEOS-Chem is a global 3-D chemical transport model for atmospheric composition driven by meteorological input data from the Goddard Earth Observing System (GEOS) of the NASA Global Modeling and Assimilation Office to simulate global atmospheric composition, including CO_2 (Bey et al., 2001). Estimates of CO_2 fluxes due to fossil fuel emissions, ocean-atmosphere exchange and biosphere-atmosphere exchange are provided by inventories and atmospheric inverse models. In the standard version of the GEOS-Chem CO_2 simulation, described by Nassar et al. (2010), CASA is used to estimate the balanced atmosphere-biosphere exchange (Olsen and Randerson, 2004).

In this study, we use GEOS-Chem version v9-01-01 with the GEOS-5 fields, and a spatial resolution of $2^{\circ} \times 2.5^{\circ}$ (latitude × longitude) with 47 vertical layers. The CO_2 simulation relies on the inventories listed in Table 1. The CO_2 simulations were started on the 1 January 2005, allowing one year spin-up for the time period 2006–2010.

In GEOS-Chem the NEE consists of two components: the first component is the net yearly uptake, based on the TransCom climatology and approximated by −5.29 PgC per year (Baker et al., 2006). The second component is the NEE disregarding the net yearly CO_2 uptake, the balanced NEE, driving the seasonal CO_2 cycle. This balanced NEE is the focus of this study and in the following sections referred to as NEE. It will be approximated with three different biosphere models, described in the following sections.

3 CASA

The Carnegie-Ames-Stanford Approach (CASA) model is the standard biosphere model input in GEOS-Chem CO_2 simulations. Three-hourly net ecosystem production (NEP) fields are computed from the difference between the gross primary production (GPP) and the respiration R_e. Monthly GPP data with a $1^{\circ} \times 1^{\circ}$ (latitude × longitude) spatial resolution are defined as two times the net primary production (NPP) derived

ACPD
12, 12759–12800, 2012

with the CASA model and scaled to 5.5° × 5.5° grid boxes. The monthly GPP values are distributed with shortwave radiation flux data from the National Center for Environmental Prediction (NCEP, Kalnay et al., 1996) data assimilation model for the year 2000 to 3-hourly values. Monthly respiration R_e data are calculated with NCEP temperature data for the year 2000 at 5.5° × 5.5° grid boxes and also interpolated to 3-h intervals (Olsen and Randerson, 2004; Potter et al., 1993).

The GEOS-Chem CO_2 simulation uses the CASA NEE interpolated to the 2° × 2.5° (latitude × longitude) GEOS-Chem grid. Hence, the standard NEE is based on data derived for the year 2000, and GEOS-Chem does not account for any interannual variability, for instance due to droughts or fire.

4 SiB

The Simple Biosphere model (SiB) parameterizes land surface biophysical processes and ecosystem metabolism (Sellers et al., 1986, 1996; Denning et al., 1996). We use 3-hourly reanalysis data of air temperature, pressure, humidity, wind speed, radiation and precipitation from the Modern-Era Retrospective analysis for Research Applications (MERRA) (Rienecker et al., 2011) to drive the model for years 2006 through 2010. Model parameters are determined using a combination of satellite data, literature values and standard SiB parameters (Sellers et al., 1996). The SiB surface fluxes are calculated at 1° × 1.25° (latitude × longitude) spatial resolution, saved as three-hour averages and scaled to the 2° × 2.5° (latitude × longitude) GEOS-Chem grid. By using MERRA data, SiB accounts for interannual variability, which is in contrast to the CASA NEE estimations. Further details on the SiB NEE simulations are given in Parazoo et al. (2008).

ACPD
12, 12759–12800, 2012

5 GBiome-BGC

GBIOME-BGCv1 is based on the BIOME-BGC numerical ecosystem model (v. 4.1.1), but is designed for global simulations (Trusilova and Churkina, 2008). BIOME-BGC is a numerical model designed for point studies in forests. It simulates water storage and fluxes, and carbon and nitrogen storage. It is parameterized for seven different types of ecosystems. The Numerical Terradynamic Simulation Group (NTSG) at the University of Montana, USA stores and updates code versions of BIOME-BGC for public release (http://www.ntsg.umt.edu/).

Daily averaged meteorological fields from the NCEP are used to derive year-specific NEE data with a $1^{\circ} \times 1^{\circ}$ spatial resolution. To modulate a diurnal CO_2 cycle, 3-hourly balanced NEE data are derived by distributing the daily GPP output per grid cell according to the solar zenith angle, whereas the respiration is linearly interpolated (Rödenbeck, 2005). Like the SiB estimations, GBiome-BGC accounts for interannual NEE variability. However, in this study the NEE estimations for the year 2009, scaled to the $2^{\circ} \times 2.5^{\circ}$ (latitude × longitude) GEOS-Chem grid, are used for the whole time period. It should be noted that the GBiome-BGC NEE estimations are not balanced, and have a net yearly uptake of $-0.705\,\mathrm{Pg\,yr^{-1}}$, in contrast to the balanced CASA and SiB models (Table 2). Therefore, the GEOS-Chem CO_2 simulations using the GBiome-BGC NEE estimations are detrended to compensate for the net yearly uptake.

6 TCCON

The Total Carbon Column Observing Network (TCCON) is a worldwide network of ground-based Fourier Transform Spectrometers (FTSs) that was founded in 2004 (Washenfelder et al., 2006). TCCON data products are column-averaged dry-air mole fractions, e.g. X_{CO_2}, X_{CH_4}, X_{N_2O}, X_{CO} (Wunch et al., 2011a). TCCON has been largely used as a calibration and validation resource for satellite measurements (e.g., Buchwitz et al., 2006; Barkley et al., 2007; Butz et al., 2011; Morino et al., 2011; Reuter

ACPD
12, 12759–12800, 2012
Evaluation of atmosphere-biosphere exchange estimations
J. Messerschmidt et al.

et al., 2011; Wunch et al., 2011b; Schneising et al., 2012) and provided insights into carbon cycle science (e.g., Yang et al., 2007; Keppel-Aleks et al., 2012). The individual TCCON sites are operated by various institutions around the world (e.g., Washenfelder et al., 2006; Deutscher et al., 2010; Geibel et al., 2010; Messerschmidt et al., 2011b; Wunch et al., 2011a). Here, TCCON X_{CO_2} data are used to analyze the influence of the three different NEE estimations on the GEOS-Chem CO_2 simulation. The TCCON X_{CO_2} data have a precision better than 0.25 % (~1 ppm) ($1-\sigma$) (Wunch et al., 2011a), under clear sky conditions, though 0.1 % ($1-\sigma$) precision can be achieved (Washenfelder et al., 2006; Deutscher et al., 2010; Messerschmidt et al., 2010). Here, X_{CO_2} measurements at the TCCON sites Bremen (Germany), Białystok (Poland), Lamont (Oklahoma) and Park Falls (Wisconsin) are used. The Park Falls and Bremen sites have the longest data records, covering the whole time period from 2006 to 2010. Measurements at Lamont started in July 2008 and in Białystok in March 2009. The data density is dependent on whether the TCCON instrument performs measurements automatically (Park Falls, Lamont and Białystok) and on the weather conditions at the site. Larger time periods without measurements indicate major instrumental failures. The numbers of days averaged in the analyses are given in Table 5. All sites were calibrated to World Metereological Organization (WMO) standards through high altitude aircraft campaigns (Wunch et al., 2010; Messerschmidt et al., 2011b) and are further introduced in Table 3.

In order to compare the GEOS-Chem CO_2 profile data with the TCCON data, they have to be integrated to column-averaged CO_2 dry-air mole fractions. We do this by applying the TCCON averaging kernels and a priori profiles to the model, employing the method developed by Rodgers and Connor (2003). For each TCCON measurement, the daily averaged GEOS-Chem CO_2 simulation profile for the same day was smoothed with the averaging kernel and a priori profile from the TCCON measurement and integrated to column averaged $X_{CO_2,\mathrm{model}}$. For the integration we use the GFIT a priori pressure, altitude, temperature and H_2O profile, which are the NCEP data interpolated to the location of the TCCON station and to local noon (Wunch et al., 2011a).

7 GEOS-Chem CO_2 simulations with different NEE estimations

The NEE estimations of the three models, CASA, SiB (2009 only) and GBiome-BGC, are shown in Fig. 1. In the upper panel, the latitudinal NEE distributions, integrated for the months May to August, are depicted. The large CO_2 sink in boreal forests (between 30° and 75° N) is evident in all three models. Nevertheless, the largest difference between the models can also be found in this region. Both SiB and GBiome-BGC exhibit a sink larger than CASA by up to 40 %. As GBiome-BGC is not balanced and a large portion of the sink can be attributed to the net yearly uptake of $-0.705\,\mathrm{Pg\,yr^{-1}}$, the sink in SiB and GBiome-BGC is dissimilar. The seasonal CO_2 cycle is mostly dominated by the NEE in the boreal forest and the biggest differences (up to 40 %) between the models are found in this region as well. Thus, our analyses focus on this region.

In the bottom panel, the time series of the monthly NEE integrated over all grid points between 30° N and 90° N ($<\mathrm{NEE}>_{30-90,\mathrm{model}}$) are compared. The time series reflect the differences already seen in the latitudinal NEE distributions: the pronounced summer sink in both SiB and GBiome-BGC leads to a larger seasonal cycle amplitude than in CASA. The winter NEE peak is unique for all three models: In January, CASA shows a dip, in contrast to the maximum in GBiome-GBC and the slightly earlier maximum in SiB. The CO_2 drawdown starts in April in GBiome-BGC and SiB and is shifted one month later in CASA. The autumn release occurs simultaneously in SiB and CASA, and about a month earlier in GBiome-BGC. These differences lead to the widest seasonal cycle minimum in SiB and narrower widths in CASA and GBiome-BGC. CASA lags GBiome-BGC by about a month.

To evaluate the differences in the GEOS-Chem CO_2 simulations using these different NEE inputs, the simulated monthly mean CO_2 between 30° and 90° N at the vertical layer of 700 hPa ($<CO_2>_{30-90,\mathrm{model}}$) is shown in the upper panel of Fig. 2. The CO_2 abundance at 700 hPa represents the free troposphere abundance and is less sensitive to local influences (Keppel-Aleks et al., 2011). The most obvious feature is that the amplitude and phase of the simulated seasonal CO_2 cycle is dominated by the dif-

ACPD
12, 12759–12800, 2012

ferences in the NEE estimations (Fig. 1). The drawdown starts about a month earlier using SiB or GBiome-BGC, in contrast to the CASA input. The largest drawdown is found for the SiB NEE and the smallest using the CASA NEE. The growing season is longest for SiB and shortest for CASA.

In the bottom panel, the monthly mean CO_2 at 700 hPa is shown averaged over four TCCON sites: Białystok (Poland), Bremen (Germany), Lamont (Oklahoma), and Park Falls (Wisconsin) ($<CO_2>_{TCCON,model}$). All four TCCON sites lie between 30° and 90° N (Table 3). The same differences as described for the CO_2 simulations integrated over nearly the entire Northern Hemisphere (upper panel) can be seen. This implies that studying these differences at the four TCCON sites gives information about the GEOS-Chem CO_2 simulation for nearly the entire Northern Hemisphere.

7.1 Evaluating GEOS-Chem CO_2 simulations with TCCON measurements

The differences between the CO_2 simulations using CASA and SiB at the four TCCON sites are as large as 0.8 % and between CASA and detrended simulations using GBiome-BGC are as large as 0.9 % (Table 4). With a precision better than 0.25 % (~ 1 ppm), TCCON total CO_2 column measurements are suitable to validate these differences.

In Fig. 3, the monthly averages of the $X_{CO_2,model}$ are compared to the mean of the monthly averages of the X_{CO_2} time series at the four TCCON sites. Comparing the $X_{CO_2,model}$ values reveals the same yearly pattern as seen for the GEOS-Chem CO_2 simulations at 700 hPa (Fig. 2). Comparing the $X_{CO_2,model}$ with the TCCON measurements reveals an underestimation of the seasonal amplitude for the simulations using GBiome-BGC and CASA and an overestimation by SiB. Using CASA, the start of the growing season is delayed for all years. The start of the growing season in SiB and GBiome-BGC is in relatively good agreement with the TCCON data.

In order to analyze these findings in more detail, the monthly means of the five years were averaged to give a mean seasonal cycle for each NEE input as well as for the TCCON data (Fig. 4). The start of the CO_2 drawdown in spring and the start of the

ACPD
12, 12759–12800, 2012

CO_2 release in autumn are estimated by the turning points of the seasonal CO_2 cycle, indicated by dots and dashed lines in in Fig. 4. The delay of the onset and the ending of the growing season are calculated by the time lag between the turning points of the simulated seasonal CO_2 cycle and the turning points of the TCCON time series. For the GEOS-Chem CO_2 simulation using SiB or GBiome-BGC, the CO_2 drawdown starts too early (with a lag of −6 days ± 1 day and −16 days ± 1 day, respectively), whereas the standard CASA NEE inventory leads to a delay in the CO_2 drawdown (by +10 days ± 1 day). In contrast, the CO_2 release is estimated to be too early using the CASA inventory (by −3 days ± 1 day), but is delayed using SiB or GBiome-BGC NEE inputs (by +9 days ± 1 day for both models). The time lags in days are given in Table 6 as well.

This estimation of the CO_2 drawdown and release relies only on the turning points. The entire seasonal cycle shape can be evaluated in a cross-correlation of the modeled X_{CO_2} and the measured TCCON X_{CO_2} (Fig. 5). The cross-correlation is a measure of the similarity of two waveform patterns as a function of a time shift applied to one waveform. The cross-correlation of the GEOS-Chem CO_2 simulation infers a time shift of −4 days ± 1 day for CASA and +4 days ± 1 day for GBiome-BGC. The simulation using SiB is optimized without shifting. The time shifts in days are also listed in Table 6.

The seasonal amplitude differences are estimated by taking the ratio of the amplitude from the GEOS-Chem CO_2 simulations and the amplitude measured by the TCCON instruments. The amplitude is calculated by the difference between the maximum and the minimum X_{CO_2} in the seasonal cycle curve. Both CASA and GBiome-BGC simulate amplitudes that are too small by 15 % and 12 %, respectively and the SiB simulation has a seasonal cycle that is too large by 9 % (Table 6).

The GEOS-Chem CO_2 simulation using the SiB model provides the best match to the measured seasonal cycle. The time delay in the CO_2 drawdown is the shortest, at −6 ± 1 days, and the cross-correlation is maximized for the unshifted simulated seasonal cycle. The time delay of the CO_2 release reveals a seasonal cycle minimum that is slightly too wide, but overall the seasonal amplitude matches the measurements well.

ACPD
12, 12759–12800, 2012

7.2 GEOS-Chem CO_2 simulation using manipulated CASA NEE estimations

The comparison of the GEOS-Chem CO_2 simulation using CASA NEE estimations with the TCCON measurements revealed a delay in the start of the growing season and a seasonal amplitude, that was too small (Fig. 4). Keppel-Aleks et al. (2012) demonstrated that a GCM simulation could be significantly improved by enhancing NEE in the boreal forest by 40 % and an earlier onset of the growing season. Here, the CASA NEE was amplified by 40 % between 45° N and 65° N and the onset of the growing season was shifted earlier by adding the NEE in July to the NEE in May between 50° N and 60° N, analogous to Keppel-Aleks et al. (2012). The resulting GEOS-Chem CO_2 simulation was detrended by 1.081 Pg yr^{-1} to account for the increased NEE uptake.

Figure 6 shows the monthly averages of the GEOS-Chem CO_2 simulation using the original CASA NEE estimations, as already depicted in Fig. 3, and the GEOS-Chem CO_2 simulation using CASA NEE estimations, manipulated as described above. The seasonal amplitude increased significantly and even overestimates the seasonal CO_2 cycle amplitude measured by the TCCON sites. The onset of the growing season seems to be in agreement with the TCCON measurements. In order to quantify the changes, the data are analyzed in an analogous fashion to the analysis in Sect. 7.1. Figure 7, like Fig. 4, shows the averages of the modeled data and the TCCON data for 2006 through 2010. The seasonal amplitude is overestimated by a factor of 1.20 (Table 6). The onset and the time period of the growing season are estimated accurately. The values of −1 ± 1 day and +2 ± 1 days for the CO_2 drawdown and release delays are a significant improvement, and the cross-correlation optimization yields an unchanged CO_2 seasonal cycle (Table 6). The calculation of the correlation coefficient between the $X_{CO_2,CASA}$ and the TCCON data improved from 0.954 to 0.963 for the manipulated $X_{CO_2,CASA}$.

These results are consistent with the findings of Keppel-Aleks et al. (2011): the NEE in the boreal forest dominates the amplitude of the seasonal CO_2 cycle and the onset time of the growing season determines the phase of the seasonal CO_2 cycle. Small

ACPD
12, 12759–12800, 2012

Title Page
Abstract | Introduction
Conclusions | References
Tables | Figures
◀| |▶
◀ ▶
Back | Close
Full Screen / Esc
Printer-friendly Version
Interactive Discussion

changes in these quantities significantly influence the seasonal CO_2 cycle measured at single locations in the Northern Hemisphere. Hence, the CO_2 distribution on synoptic scales drives local variability in atmospheric total column CO_2.

7.3 Impact of year-specific NEE fluxes on the GEOS-Chem CO_2 simulation

The GEOS-Chem CO_2 simulations with CASA and GBiome-BGC were performed with the same NEE estimates for each year. SiB, however, has year-specific meteorology, and so the SiB NEE changes every year. In order to quantify the difference between the year-specific NEE and the static NEE, a simulation for 2006 through 2010 was calculated using the SiB NEE estimation for the year 2009. This approach gives a measure for the difference between the climatology and year-specific fluxes.

Figure 8 shows the monthly averages of the GEOS-Chem CO_2 simulation using year-specific NEE estimations, as already depicted in Fig. 3, and the GEOS-Chem CO_2 simulation using SiB 2009 NEE estimations for the entire time period. Both simulations show only slight differences. The scatter plot of $X_{CO_2,SiB2009NEE}$, $X_{CO_2,SiB}$ and $X_{CO_2,CASA}$ against the TCCON data is shown in Fig. 9 and the correlation coefficients are given in Table 7 with 0.971 for year-specific SiB NEE estimates and 0.970 for SiB 2009 NEE estimations. These findings show that the year-specific NEE only slightly improves the agreement with the measured seasonal cycle, suggesting that the CO_2 seasonal cycle is mainly driven by the spatial flux distribution and the atmospheric dynamics.

In summary, the analyses highlight good performance for all three models, with the best fit given by the SiB NEE estimates calculated with the specific yearly meteorology.

8 Improved NEE inventory for the GEOS-Chem CO_2 simulation

GEOS-Chem CO_2 simulations using year-specific SiB NEE estimations are a significant improvement compared to simulations with the standard CASA climatology. To illustrate the differences between the standard CASA climatology and the SiB yearly val-

ACPD
12, 12759–12800, 2012

ues, we follow the method described by Nassar et al. (2010) in comparing the GEOS-Chem CO_2 simulations using SiB with the GLOBALVIEW measurements of the surface CO_2 concentrations and to the individual TCCON time series used in the analyses in Sect. 7.

8.1 Comparison with TCCON measurements

In Fig. 10 the TCCON X_{CO_2} time series at the four TCCON sites used in this study, Park Falls (Wisconsin), Lamont (Oklahoma), Bremen (Germany), and Białystok (Poland) are compared with GEOS-Chem CO_2 simulations using CASA and SiB NEE.

The findings from Sect. 7 are evident in the comparisons of the individual time series. The seasonal cycle of the GEOS-Chem CO_2 simulations using SiB estimations fits the data best when comparing the measured and modeled seasonal cycle amplitude and phase. The GEOS-Chem CO_2 simulations using CASA inputs tend to underestimate the CO_2 abundance, especially in the seasonal cycle minimum, and the seasonal cycle phase is often delayed compared to the TCCON measurements.

8.2 Comparison with GLOBALVIEW-CO2 data

The GLOBALVIEW-CO2 data (GLOBALVIEW-CO2, 2011) are maintained by the Carbon Cycle Greenhouse Gases Group of the National Oceanic and Atmospheric Administration, Earth System Research Laboratory (NOAA ESRL) within the Cooperative Atmospheric Data Integration Project. They are derived (as described by Masarie and Tans, 1995) from highly precise atmospheric CO_2 measurements and widely used for atmospheric model validation. The GEOS-Chem CO_2 simulations using the standard CASA input and the SiB fluxes are compared to GLOBALVIEW-CO2 data at 30 sampling sites. The sampling sites were chosen so as to cover the whole latitude range (82° N to 90° S) and to be comparable to the study by Nassar et al. (2010), which introduces the current version of the GEOS-Chem CO_2 simulation.

ACPD
12, 12759–12800, 2012

In Fig. 11, the GLOBALVIEW-CO2 data are shown in addition to the weekly averages of the simulated model concentrations at the sampling site altitude for the years 2006 to 2010. The seasonal amplitude is always larger using SiB fluxes than using CASA fluxes, and tends to over- and underestimate the seasonal maximum and minimum in the Northern Hemisphere measurements. In the Southern Hemisphere, the use of SiB fluxes leads to simulation of lower CO_2 in contrast to the use of CASA estimations. Figure 12 shows the differences between the model and the GLOBALVIEW-CO2 data for all 30 measurement sites. The mean differences for the CO_2 simulations are 0.92 ppm and 0.61 ppm using CASA and SiB, respectively.

9 Conclusions

We evaluated three estimations of biosphere fluxes within the chemical transport model GEOS-Chem. Errors in the global CO_2 distribution could be analyzed through comparison with TCCON measurements. The standard GEOS-Chem CO_2 simulation (Nassar et al., 2010) uses CASA NEE to estimate the balanced atmosphere-biosphere exchange. However, we show that the estimate of the CO_2 uptake in the growing season in the boreal forest is underestimated and that the onset of the growing season is delayed using this estimate of biospheric fluxes. By enhancing the CO_2 uptake in the boreal forest and shifting the onset of the growing season earlier, the comparison with TCCON data is significantly improved. Similar to CASA, GBiome-BGC also underestimates the CO_2 uptake in the growing season. SiB shows reasonably good agreement in comparison with the TCCON data.

The accurate estimation of carbon fluxes is crucial for the correct simulation of the carbon cycle. The inconsistency of some atmospheric inverse model results with vertical aircraft profiles and total column measurements shown in recent studies reveal a general problem in inverse estimates of carbon fluxes (e.g., Stephens et al., 2007). The inverse machinery must span hemispheric scales, otherwise errors in the inferred distribution at one spatial scale can alias into errors at other spatial scales. Variability in

Discussion Paper | Discussion Paper | Discussion Paper | Discussion Paper |

ACPD

12, 12759–12800, 2012

Evaluation of atmosphere-biosphere exchange estimations

J. Messerschmidt et al.

local CO_2 concentrations is affected even by variations in the CO_2 distribution on hemispheric scale. This means that atmospheric inverse modeling must extend globally to retrieve fluxes.

Additionally, errors on a synoptic scale must be carefully evaluated before retrieving local fluxes. Variations in the total column are a good validation resource for diagnosing errors in the hemispheric scale in the estimates of these fluxes, because they provide information on the largest scales. We suggest that an inverse model designed to retrieve the north-south distribution of the fluxes from total column measurements and local fluxes from in situ surface sampling would be helpful.

Acknowledgements. We thank Ray Nassar (Environment Canada) for his helpful support and the committed discussions. This analysis was supported by a sub-contract from University of California, Irvine (NASA NNX10AT83G, James Randerson, PI). For the TCCON sites at Białystok (Poland) we acknowledge financial support by the Senate of Bremen and the EU projects IMECC and GEOmon as well as maintainance and logistical work provided by AeroMeteo Service (Białystok). Support for the US TCCON operations is provided by NASA's Carbon Cycle Program grant NNX11AG016 for Park Falls (Wisconsin), and NASA's ACOS/OCO-2 project for Lamont (Oklahoma). The simulations used in this study were performed on the Caltech Division of Geological and Planetary Sciences Dell Cluster. GBIOME-BGCv1 is provided by the Max-Planck Institute for Biogeochemistry, Germany. MPI assumes no responsibility for the proper use of GBIOME-BGC by others.

References

Andres, R. J., Marland, G., Fung, I., and Matthews, E.: A 1 × 1 distribution of carbon dioxide emissions from fossil fuel consumption and cement manufacture, 1950–1990, Global Biogeochem. Cy., 10, 419–429, doi:10.1029/96GB01523, 1996. 12782

Baker, D. F., Law, R. M., Gurney, K. R., Rayner, P., Peylin, P., Denning, A. S., Bousquet, P., Bruhwiler, L., Chen, Y.-H., Ciais, P., Fung, I. Y., Heimann, M., John, J., Maki, T., Maksyutov, S., Masarie, K., Prather, M., Pak, B., Taguchi, S., and Zhu, Z.: TransCom 3 inversion intercomparison: impact of transport model errors on the interannual variability of regional

ACPD
12, 12759–12800, 2012

CO_2 fluxes, 1988–2003, Global Biogeochem. Cy., 20, GB1002, doi:10.1029/2004GB002439, 2006. 12760, 12763, 12782

Baker, I., Denning, A. S., Hanan, N., Prihodko, L., Uliasz, M., Vidale, P.-L., Davis, K., and Bakwin, P.: Simulated and observed fluxes of sensible and latent heat and CO_2 at the WLEF-TV Tower using SiB2.5, Global Change Biol., 9, 1262–1277, 2003. 12762

Barkley, M. P., Monks, P. S., Hewitt, A. J., Machida, T., Desai, A., Vinnichenko, N., Nakazawa, T., Yu Arshinov, M., Fedoseev, N., and Watai, T.: Assessing the near surface sensitivity of SCIAMACHY atmospheric CO_2 retrieved using (FSI) WFM-DOAS, Atmos. Chem. Phys., 7, 3597–3619, doi:10.5194/acp-7-3597-2007, 2007. 12765

Bey, I., Jacob, D. J., Yantosca, R. M., Logan, J. A., Field, B., Fiore, A. M., Li, Q., Liu, H., Mickley, L. J., and Schultz, M.: Global modeling of tropospheric chemistry with assimilated meteorology: model description and evaluation, J. Geophys. Res., 106, 23073–23096, 2001. 12763

Boden, T., Marland, G., and Andres, R.: Global, Regional, and National Fossil-Fuel CO_2 Emissions, Tech. rep., Carbon Dioxide Information Analysis Center, Oak Ridge National Laboratory, US Department of Energy, Oak Ridge, Tenn., USA, doi:10.3334/CDIAC/00001, 2009. 12782

Buchwitz, M., de Beek, R., Noël, S., Burrows, J. P., Bovensmann, H., Schneising, O., Khlystova, I., Bruns, M., Bremer, H., Bergamaschi, P., Körner, S., and Heimann, M.: Atmospheric carbon gases retrieved from SCIAMACHY by WFM-DOAS: version 0.5 CO and CH_4 and impact of calibration improvements on CO_2 retrieval, Atmos. Chem. Phys., 6, 2727–2751, doi:10.5194/acp-6-2727-2006, 2006. 12765

Butz, A., Guerlet, S., Hasekamp, O., Schepers, D., Galli, A., Aben, I., Frankenberg, C., Hartmann, J., Tran, H., Kuze, A., Keppel-Aleks, G., Toon, G., Wunch, D., Wennberg, P., Deutscher, N., Griffith, D., Macatangay, R., Messerschmidt, J., Notholt, J., and Warneke, T.: Toward accurate CO_2 and CH_4 observations from GOSAT, Geophys. Res. Lett., 38, L14812, doi:10.1029/2011GL047888, 2011. 12765

Corbett, J. J. and Koehler, H. W.: Considering alternative input parameters in an activity-based ship fuel consumption and emissions model: reply to comment by Endresen et al. on “Updated emissions from ocean shipping”, J. Geophys. Res., 109, D23303, doi:10.1029/2004JD005030, 2004. 12782

Corbett, J. J. and Koehler, H. W.: Updated emissions from ocean shipping, J. Geophys. Res., 108, 4650, doi:10.1029/2003JD003751, 2003. 12782

ACPD
12, 12759–12800, 2012

Evaluation of atmosphere-biosphere exchange estimations

J. Messerschmidt et al.

Title Page
Abstract | Introduction
Conclusions | References
Tables | Figures
◀| |▶
◀ ▶
Back | Close
Full Screen / Esc
Printer-friendly Version
Interactive Discussion

Denning, A. S., Collatz, G. J., Zhang, C., Randall, D. A., Berry, J. A., Sellers, P. J., Colello, G. D., and Dazlich, D. A.: Simulations of terrestrial carbon metabolism and atmospheric CO_2 in a general circulation model. Part 1: Surface carbon fluxes, Tellus B, 48, 521–542, 1996. 12764

Deutscher, N. M., Griffith, D. W. T., Bryant, G. W., Wennberg, P. O., Toon, G. C., Washenfelder, R. A., Keppel-Aleks, G., Wunch, D., Yavin, Y., Allen, N. T., Blavier, J.-F., Jiménez, R., Daube, B. C., Bright, A. V., Matross, D. M., Wofsy, S. C., and Park, S.: Total column CO_2 measurements at Darwin, Australia – site description and calibration against in situ aircraft profiles, Atmos. Meas. Tech., 3, 947–958, doi:10.5194/amt-3-947-2010, 2010. 12766

Endresen, O., Sorgard, E., Behrens, H. L., Brett, P. O., and Isaksen, I. S. A.: A historical reconstruction of ships' fuel consumption and emissions, J. Geophys. Res., 112, D12301, doi:10.1029/2006JD007630, 2007. 12782

Gaudinski, J. B., Trumbore, S., Davidson, E., and Zheng, S.: Soil carbon cycling in a temperate forest: radiocarbon-based estimated of residence times, sequestration rates and partitioning of fluxes, Biogeochemistry, 51, 33–69, 2000. 12760

Geibel, M. C., Gerbig, C., and Feist, D. G.: A new fully automated FTIR system for total column measurements of greenhouse gases, Atmos. Meas. Tech., 3, 1363–1375, doi:10.5194/amt-3-1363-2010, 2010. 12766

GLOBALVIEW-CO2: Cooperative Atmospheric Data Integration Project – Carbon Dioxide, NOAA-ESRL, Boulder, Colorado, CD-ROM, 2011. 12762, 12772

Goodale, C. L., Apps, M. J., Birdsey, R. A., Field, C. B., Heath, L. S., Houghton, R. A., Jenkins, J. C., Kohlmaier, G. H., Kurz, W., Liu, S., Nabuurs, G.-J., Nilsson, S., and Shvidenko, A. Z.: Forest carbon sinks in the Northern Hemisphere, Ecol. Appl., 12, 891–899, doi:10.1890/1051-0761(2002)012[0891:FCSITN]2.0.CO;2, 2002. 12760

Kalnay, E., Kanamitsu, M., Kistler, R., Collins, W., Deaven, D., Gandin, L., Iredell, M., Saha, S., White, G., Woollen, J., Zhu, Y., Leetmaa, A., Reynolds, R., Chelliah, M., Ebisuzaki, W., Higgins, W., Janowiak, J., Mo, K. C., Ropelewski, C., Wang, J., Jenne, R., and Joseph, D.: The NCEP/NCAR 40-year reanalysis project, B. Am. Meteorol. Soc., 77, 437–471, doi:10.1175/1520-0477, 1996. 12764

Keppel-Aleks, G., Wennberg, P. O., and Schneider, T.: Sources of variations in total column carbon dioxide, Atmos. Chem. Phys., 11, 3581–3593, doi:10.5194/acp-11-3581-2011, 2011. 12761, 12762, 12767, 12770

Keppel-Aleks, G., Wennberg, P. O., Washenfelder, R. A., Wunch, D., Schneider, T., Toon, G. C., Andres, R. J., Blavier, J.-F., Connor, B., Davis, K. J., Desai, A. R., Messerschmidt, J., Notholt, J., Roehl, C. M., Sherlock, V., Stephens, B. B., Vay, S. A., and Wofsy, S. C.: The imprint of surface fluxes and transport on variations in total column carbon dioxide, Biogeosciences, 9, 875–891, doi:10.5194/bg-9-875-2012, 2012. 12761, 12766, 12770

Kim, B. Y., Fleming, Gregg, G., Balasubramanian, S., Malwitz, A., Klima, K., Locke, M., Holsclaw, C. A., Maurice, L. Q., and Gupta, M. L.: System for assessing Aviations Global Emissions (SAGE) Version 1.5 global Aviation Emissions Inventories for 2000–2004, Tech. rep., The United States Federal Aviation Administration (FAA) Office of Environment and Energy (AEE), 2005. 12782

Kim, B. Y., Fleming, Gregg, G., Lee, J. J., Waitz, I. A., Clarke, J.-P., Balasubramanian, S., Malwitz, A., Klima, K., Locke, M., Holsclaw, C. A., Maurice, L. Q., and Gupta, M. L.: System for assessing Aviations Global Emissions (SAGE), Part 1: Model description and inventory results, Transport. Res. D-Tr. E., 12, 325–346, doi:10.1016/j.trd.2007.03.007, 2007. 12782

Le Quere, C., Raupach, M. R., Canadell, J. G., and Marland, G.: Trends in the sources and sinks of carbon dioxide, Nat. Geosci., 2, 831–836, doi:10.1038/ngeo689, 2009. 12782

Masarie, K. and Tans, P.: Extension and integration of atmospheric carbon dioxide data into a globally consistent measurement record, J. Geophys. Res., 100, 11593–11610, 1995. 12772

Messerschmidt, J., Macatangay, R., Notholt, J., Petri, C., Warneke, T., and Weinzierl, C.: Side by side measurements of CO_2 by ground-based Fourier transform spectrometry (FTS), Tellus B, 62, 749–758, doi:10.1111/j.1600-0889.2010.00491.x, 2010. 12766

Messerschmidt, J., Chen, H., Deutscher, N. M., Gerbig, C., Grupe, P., Katrynski, K., Koch, F.-T., Lavrič, J. V., Notholt, J., Rödenbeck, C., Ruhe, W., Warneke, T., and Weinzierl, C.: Automated ground-based remote sensing measurements of greenhouse gases at the Białystok site in comparison with collocated in-situ measurements and model data, Atmos. Chem. Phys. Discuss., 11, 32245–32282, doi:10.5194/acpd-11-32245-2011, 2011a. 12784

Messerschmidt, J., Geibel, M. C., Blumenstock, T., Chen, H., Deutscher, N. M., Engel, A., Feist, D. G., Gerbig, C., Gisi, M., Hase, F., Katrynski, K., Kolle, O., Lavrič, J. V., Notholt, J., Palm, M., Ramonet, M., Rettinger, M., Schmidt, M., Sussmann, R., Toon, G. C., Truong, F., Warneke, T., Wennberg, P. O., Wunch, D., and Xueref-Remy, I.: Calibration of TCCON column-averaged CO_2: the first aircraft campaign over European TCCON sites, Atmos. Chem. Phys., 11, 10765–10777, doi:10.5194/acp-11-10765-2011, 2011b. 12766

Michalak, A. M., Bruhwiler, L., and Tans, P. P.: A geostatistical approach to surface flux estimation of atmospheric trace gases, J. Geophys. Res., 109, D14109, doi:10.1029/2003JD004422, 2004. 12760

Morino, I., Uchino, O., Inoue, M., Yoshida, Y., Yokota, T., Wennberg, P. O., Toon, G. C., Wunch, D., Roehl, C. M., Notholt, J., Warneke, T., Messerschmidt, J., Griffith, D. W. T., Deutscher, N. M., Sherlock, V., Connor, B., Robinson, J., Sussmann, R., and Rettinger, M.: Preliminary validation of column-averaged volume mixing ratios of carbon dioxide and methane retrieved from GOSAT short-wavelength infrared spectra, Atmos. Meas. Tech., 4, 1061–1076, doi:10.5194/amt-4-1061-2011, 2011. 12765

Nassar, R., Jones, D. B. A., Suntharalingam, P., Chen, J. M., Andres, R. J., Wecht, K. J., Yantosca, R. M., Kulawik, S. S., Bowman, K. W., Worden, J. R., Machida, T., and Matsueda, H.: Modeling global atmospheric CO_2 with improved emission inventories and CO_2 production from the oxidation of other carbon species, Geosci. Model Dev., 3, 689–716, doi:10.5194/gmd-3-689-2010, 2010. 12763, 12772, 12773, 12782

Olsen, S. C. and Randerson, J. T.: Differences between surface and column atmospheric CO_2 and implications for carbon cycle research, J. Geophys. Res., 109, D02301, doi:10.1029/2003JD003968, 2004. 12762, 12763, 12764, 12782

Parazoo, N. C., Denning, A. S., Kawa, S. R., Corbin, K. D., Lokupitiya, R. S., and Baker, I. T.: Mechanisms for synoptic variations of atmospheric CO_2 in North America, South America and Europe, Atmos. Chem. Phys., 8, 7239–7254, doi:10.5194/acp-8-7239-2008, 2008. 12761, 12764

Peters, W., Jacobson, A. R., Sweeney, C., Andrews, A. E., Conway, T. J., Masarie, K., Miller, J. B., Bruhwiler, L. M. P., Pétron, G., Hirsch, A. I., Worthy, D. E. J., van der Werf, G. R., Randerson, J. T., Wennberg, P. O., Krol, M. C., and Tans, P. P.: An atmospheric perspective on North American carbon dioxide exchange: CarbonTracker, P. Natl. Acad. Sci. USA, 104, 18925–18930, 2007. 12760

Potter, C. S., Randerson, J. T., Field, C. B., Matson, P. A., Vitousek, P. M., Mooney, H. A., and Klooster, S. A.: Terrestrial ecosystem production: a process model based on global satellite and surface data, Global Biogeochem. Cy., 7, 811–841, doi:10.1029/93GB02725, 1993. 12764, 12782

Rayner, P. J. and O'Brien, D. M.: The utility of remotely sensed CO_2 concentration data in surface source inversions, Geophys. Res. Lett., 28, 175–178, doi:10.1029/2000GL011912, 2001. 12761

ACPD
12, 12759–12800, 2012

Evaluation of atmosphere-biosphere exchange estimations

J. Messerschmidt et al.

Rödenbeck, C.: Estimating CO_2 sources and sinks from atmospheric mixing ratio measurements using a global inversion of atmospheric transport, Technical report 6, Max Planck Institute for Biogeochemistry, Jena, 2005. 12765
Reuter, M., Bovensmann, H., Buchwitz, M., Burrows, J. P., Connor, B. J., Deutscher, N. M., Griffith, D. W. T., Heymann, J., Keppel-Aleks, G., Messerschmidt, J., Notholt, J., Petri, C., Robinson, J., Schneising, O., Sherlock, V., Velazco, V., Warneke, T., Wennberg, P. O., and Wunch, D.: Retrieval of atmospheric CO_2 with enhanced accuracy and precision from SCIAMACHY: validation with FTS measurements and comparison with model results, J. Geophys. Res., 116, D04301, doi:10.1029/2010JD015047, 2011. 12765
Rienecker, M. M., Suarez, M. J., Gelaro, R., Todling, R., Bacmeister, J., Liu, E., Bosilovich, M. G., Schubert, S. D., Takacs, L., Kim, G.-K., Bloom, S., Chen, J., Collins, D., Conaty, A., da Silva, A., Gu, W., Joiner, J., Koster, R. D., Lucchesi, R., Molod, A., Owens, T., Pawson, S., Pegion, P., Redder, C. R., Reichle, R., Robertson, F. R., Ruddick, A. G., Sienkiewicz, M., and Woollen, J.: MERRA: NASA Modern-Era Retrospective Analysis for Research and Applications, J. Climate, 24, 3624–3648, 2011. 12764
Rodgers, C. D. and Connor, B. J.: Intercomparison of remote sounding instruments, J. Geophys. Res., 108, 4116, doi:10.1029/2002JD002299, 2003. 12766
Sausen, R. and Schumann, U.: Estimates of the climate response to aircraft CO_2 and NO_x emissions scenarios, Climatic Change, 44, 27–58, 2000. 12782
Schneising, O., Bergamaschi, P., Bovensmann, H., Buchwitz, M., Burrows, J. P., Deutscher, N. M., Griffith, D. W. T., Heymann, J., Macatangay, R., Messerschmidt, J., Notholt, J., Rettinger, M., Reuter, M., Sussmann, R., Velazco, V. A., Warneke, T., Wennberg, P. O., and Wunch, D.: Atmospheric greenhouse gases retrieved from SCIAMACHY: comparison to ground-based FTS measurements and model results, Atmos. Chem. Phys., 12, 1527–1540, doi:10.5194/acp-12-1527-2012, 2012. 12766
Sellers, P. J., Mintz, Y., Sud, Y. C., and Dalcher, A.: A simple biosphere model (sib) for use within general circulation models, J. Atmos. Sci., 43, 505–531, 1986. 12764
Sellers, P. J., Randall, D. A., Collatz, G. J., Berry, J. A., Field, C. B., Dazlich, D. A., Zhang, C., Colello, G. D., and Bounoua, L.: A revised land surface parameterization (SiB2) for atmospheric GCMs. Part I: Model formulation, J. Climate, 9, 676–705, 1996. 12764
Stephens, B. B., Gurney, K. R., Tans, P. P., Sweeney, C., Peters, W., Bruhwiler, L., Ciais, P., Ramonet, M., Bousquet, P., Nakazawa, T., Aoki, S., Machida, T., Inoue, G., Vinnichenko, N., Lloyd, J., Jordan, A., Heimann, M., Shibistova, O., Langenfelds, R. L.,

Steele, L. P., Francey, R. J., and Denning, A. S.: Weak northern and strong tropical land carbon uptake from vertical profiles of atmospheric CO_2, Science, 316, 1732–1735, doi:10.1126/science.1137004, 2007. 12773

Takahashi, T., Sutherland, S. C., Wanninkhof, R., Sweeney, C., Feely, R. A., Chipman, D. W., Hales, B., Friederich, G., Chavez, F., Sabine, C., Watson, A., Bakker, D. C., Schuster, U., Metzl, N., Yoshikawa-Inoue, H., Ishii, M., Midorikawa, T., Nojiri, Y., Körtzinger, A., Steinhoff, T., Hoppema, M., Olafsson, J., Arnarson, T. S., Tilbrook, B., Johannessen, T., Olsen, A., Bellerby, R., Wong, C., Delille, B., Bates, N., and de Baar, H. J.: Climatological mean and decadal change in surface ocean $p\mathrm{CO}_2$, and net sea-air CO_2 flux over the global oceans, Deep-Sea Res. Pt. I, 56, 554–577, doi:10.1016/j.dsr2.2008.12.009, 2009. 12782

Trusilova, K. and Churkina, G.: The terrestrial ecosystem model GBIOME-BGCv1, Technical Reports – 14, Tech. rep., Max-Planck-Institut für Biogeochemie, Jena, Germany, 2008. 12762, 12765

Wang, C., Corbett, J., and Firestone, J.: Modeling energy use and emissions from North American shipping: application of the ship traffic, energy, and environment model, Environ. Sci. Technol., 41, 3226–3232, doi:10.1021/es060752e, 2007. 12782

Washenfelder, R., Toon, G., Blavier, J.-F., Yang, Z., Allen, N., Wennberg, P., Vay, S., Matross, D., and Daube, B.: Carbon dioxide column abundances at the Wisconsin Tall Tower site, J. Geophys. Res., 111, 1–11, doi:10.1029/2006JD007154, 2006. 12765, 12766, 12784

Wilkerson, J. T., Jacobson, M. Z., Malwitz, A., Balasubramanian, S., Wayson, R., Fleming, G., Naiman, A. D., and Lele, S. K.: Analysis of emission data from global commercial aviation: 2004 and 2006, Atmos. Chem. Phys., 10, 6391–6408, doi:10.5194/acp-10-6391-2010, 2010. 12782

Wunch, D., Toon, G. C., Wennberg, P. O., Wofsy, S. C., Stephens, B. B., Fischer, M. L., Uchino, O., Abshire, J. B., Bernath, P., Biraud, S. C., Blavier, J.-F. L., Boone, C., Bowman, K. P., Browell, E. V., Campos, T., Connor, B. J., Daube, B. C., Deutscher, N. M., Diao, M., Elkins, J. W., Gerbig, C., Gottlieb, E., Griffith, D. W. T., Hurst, D. F., Jiménez, R., Keppel-Aleks, G., Kort, E. A., Macatangay, R., Machida, T., Matsueda, H., Moore, F., Morino, I., Park, S., Robinson, J., Roehl, C. M., Sawa, Y., Sherlock, V., Sweeney, C., Tanaka, T., and Zondlo, M. A.: Calibration of the Total Carbon Column Observing Network using aircraft profile data, Atmos. Meas. Tech., 3, 1351–1362, doi:10.5194/amt-3-1351-2010, 2010. 12766

ACPD
12, 12759–12800, 2012

Wunch, D., Toon, G. C., Blavier, J.-F. L., Washenfelder, R. A., Notholt, J., Connor, B. J., Griffith, D. W. T., Sherlock, V., and Wennberg, P. O.: The total carbon column observing network, Philos. T. R. Soc. A, 369, 2087–2112, doi:10.1098/rsta.2010.0240, 2011a. 12765, 12766

Wunch, D., Wennberg, P. O., Toon, G. C., Connor, B. J., Fisher, B., Osterman, G. B., Frankenberg, C., Mandrake, L., O'Dell, C., Ahonen, P., Biraud, S. C., Castano, R., Cressie, N., Crisp, D., Deutscher, N. M., Eldering, A., Fisher, M. L., Griffith, D. W. T., Gunson, M., Heikkinen, P., Keppel-Aleks, G., Kyrö, E., Lindenmaier, R., Macatangay, R., Mendonca, J., Messerschmidt, J., Miller, C. E., Morino, I., Notholt, J., Oyafuso, F. A., Rettinger, M., Robinson, J., Roehl, C. M., Salawitch, R. J., Sherlock, V., Strong, K., Sussmann, R., Tanaka, T., Thompson, D. R., Uchino, O., Warneke, T., and Wofsy, S. C.: A method for evaluating bias in global measurements of CO_2 total columns from space, Atmos. Chem. Phys., 11, 12317–12337, doi:10.5194/acp-11-12317-2011, 2011b. 12766

Yang, Z., Washenfelder, R., Keppel-Aleks, G., Krakauer, N., Randerson, J., Tans, P., Sweeney, C., and Wennberg, P.: New constraints on Northern Hemisphere growing season net flux, Geophys. Res. Lett., 34, L12807, doi:10.1029/2007GL029742, 2007. 12761, 12766

Yevich, R. and Logan, J. A.: An assessment of biofuel use and burning of agricultural waste in the developing world, Global Biogeochem. Cy., 17, 1095, doi:10.1029/2002GB001952, 2003. 12782

ACPD

12, 12759–12800, 2012

Evaluation of atmosphere-biosphere exchange estimations

J. Messerschmidt et al.

Title Page
Abstract | Introduction
Conclusions | References
Tables | Figures
◀| |▶
◀ ▶
Back | Close
Full Screen / Esc
Printer-friendly Version
Interactive Discussion

Table 1. Fluxes used in the GEOS-Chem CO_2 simulation. The inventories, a short description and references are listed as in Nassar et al. (2010).

Flux	Inventory	Description	References
Fossil fuel emissions	CDIAC	(Carbon Dioxide Information Analysis Center), Year-specific monthly averaged fossil fuel emissions, 2008–2010 scaled with CDIAC 2007 data	Andres et al. (1996), Boden et al. (2009), Le Quere et al. (2009)
Fire emissions	GFED (v.2)	(Global Fire Emissions Database), 8-day data (2001–2007)	
Biofuel emissions			Yevich and Logan (2003)
Balanced ecosystem exchange	CASA	3-hourly Net Ecosystem Production (NEP), (balanced – no net annual flux)	Potter et al. (1993); Olsen and Randerson (2004)
Net ecosystem uptake	TransCom climatology	$-5.29\,PgC\,yr^{-1}$ (adjusted for biomass/biofuel burning)	Baker et al. (2006)
Ocean exchange		Monthly ocean flux climatology of non-El Nino years	Takahashi et al. (2009)
Ship emissions	ICOADS	(International Comprehensive Ocean Atmosphere Data Set), International ship CO_2 emissions with monthly variability scaled to annual values for 1985–2006	Corbett and Koehler (2003, 2004); Wang et al. (2007); Endresen et al. (2007)
Plane emissions	SAGE	(System for assessing Aviations Global Emissions), Aviation emission 3-D distribution from fuel burning, scaled to annual CO_2 values for 1985–2002 and estimates for 2002–2009.	Sausen and Schumann (2000); Kim et al. (2005, 2007); Wilkerson et al. (2010)

ACPD
12, 12759–12800, 2012

Table 2. The net yearly uptake of the three NEE estimation models, CASA, SiB and GBiome-BGC, used in this study.

Model	Net yearly uptake ($Pg\,yr^{-1}$)
CASA	−0.002
Manipulated CASA	−1.081
SiB (2006)	−0.081
SiB (2007)	−0.063
SiB (2008)	−0.065
SiB (2009)	−0.065
SiB (2010)	−0.061
GBiome-BGC	−0.705

ACPD
12, 12759–12800, 2012

Table 3. TCCON sites (latitude, longitude and altitude). The data record time period and references are listed.

Site	Lat. (° N)	Long. (° E)	Alt. (m a.s.l.)	Data record (date)	References
Białystok, Poland	53.23	23.03	180	since Mar 2009	Messerschmidt et al. (2011a)
Bremen, Germany	53.10	8.85	5	since Mar 2005	
Lamont, Oklahoma	36.60	−97.49	320	since Jul 2008	
Park Falls, Wisconsin	45.95	−90.27	442	since Apr 2004	Washenfelder et al. (2006)

ACPD
12, 12759–12800, 2012

ACPD

12, 12759–12800, 2012

Evaluation of atmosphere-biosphere exchange estimations

J. Messerschmidt et al.

Title Page
Abstract | Introduction
Conclusions | References
Tables | Figures
Back | Close
Full Screen / Esc
Printer-friendly Version
Interactive Discussion

Table 4. Differences in the NEE estimations of SiB and GBiome-BGC in contrast to the standard CASA inventory (first row) and the differences in the GEOS-Chem CO_2 simulations, integrated between 30° N and 90° N (second row) and averaged at four TCCON sites (third row).

	SiB	GBiome-BGC
$\frac{\langle NEE\rangle_{30-90,\text{model-CASA}}}{\text{mean}(\langle NEE\rangle_{30-90,\text{ CASA}})}$	135.7–4.7 (%)	163.9–6.4 (%)
$\langle NEE\rangle_{30-90,\text{model-CASA}}$	31–1 ($\text{kg C m}^2\ \text{month}^{-1}$)	38–1 ($\text{kg C m}^2\ \text{month}^{-1}$) with net yearly uptake
$\frac{\langle CO_2\rangle_{30-90,\text{model-CASA}}}{\text{mean}(\langle CO_2\rangle_{30-90,\text{CASA}})}$	1.01–0.01 (%)	1.36–0.00 (%)
$\langle CO_2\rangle_{30-90,\text{model-CASA}}$	4–0 (ppm)	5–0 (ppm) detrended
$\frac{\langle CO_2\rangle_{\text{TCCON,model-CASA}}}{\text{mean}(\langle CO_2\rangle_{\text{TCCON,CASA}})}$	0.81–0.01 (%)	0.9–0.01 (%)
$\langle CO_2\rangle_{\text{TCCON,model-CASA}}$	3–0 (ppm)	3–0 (ppm) detrended

Table 5. Days of TCCON measurements averaged in the monthly means shown in Figs. 3, 6 and 8.

Year	Jan	Feb	Mar	Apr	May	Jun	Jul	Aug	Sep	Oct	Nov	Dec
2006												
Bi:	0	0	0	0	0	0	0	0	0	0	0	0
Br:	2	2	4	7	6	9	9	2	10	3	0	0
Oc:	0	0	0	0	0	0	0	0	0	0	0	0
Pa:	13	21	9	24	27	14	30	29	24	19	17	7
2007												
Bi:	0	0	0	0	0	0	0	0	0	0	0	0
Br:	4	1	8	9	6	1	4	4	4	5	5	1
Oc:	0	0	0	0	0	0	0	0	0	0	0	0
Pa:	5	0	8	14	12	16	27	22	16	0	0	0
2008												
Bi:	0	0	0	0	0	0	0	0	0	0	0	0
Br:	2	4	3	10	8	6	6	0	13	9	4	3
Oc:	0	0	0	0	0	0	26	30	25	27	26	12
Pa:	0	0	0	0	25	22	10	28	25	23	14	10
2009												
Bi:	0	0	5	26	18	17	23	13	5	4	5	3
Br:	5	2	7	11	12	6	5	5	5	6	1	1
Oc:	26	25	22	24	28	29	25	30	27	20	26	22
Pa:	2	7	15	20	27	24	19	28	18	17	21	15
2010												
Bi:	10	5	22	12	12	21	17	2	0	13	0	4
Br:	2	3	8	10	3	9	7	1	2	2	1	2
Oc:	20	17	26	24	25	28	29	30	27	30	26	27
Pa:	18	14	20	23	1	0	0	11	22	25	15	17

ACPD
12, 12759–12800, 2012

Table 6. Analysis of the GEOS-Chem CO_2 simulations using different NEE estimations.

	CASA	SiB	GBiome-BGC	Manipulated CASA
CO_2 drawdown time delay (days)	10 ± 1	−6 ± 1	−16 ± 1	−1 ± 1
CO_2 release time delay (days)	−3 ± 1	9 ± 1	9 ± 1	2 ± 1
Cross-correlation between The seasonal cycles (days)	−4 ± 1	0 ± 1	4 ± 1	0 ± 1
Scaling factor fitting the Seasonal amplitude (a.u.)	0.85	1.09	0.88	1.20

ACPD
12, 12759–12800, 2012

ACPD
12, 12759–12800, 2012

Evaluation of atmosphere-biosphere exchange estimations

J. Messerschmidt et al.

Table 7. Correlation coefficients for GEOS-Chem CO_2 simulations with TCCON measurements for the standard CASA inventory, year-specific SiB fluxes and SiB climatology.

	CASA	SiB	SiB 2009 NEE	Manipulated CASA
Correlation coefficient	0.954	0.971	0.970	0.963

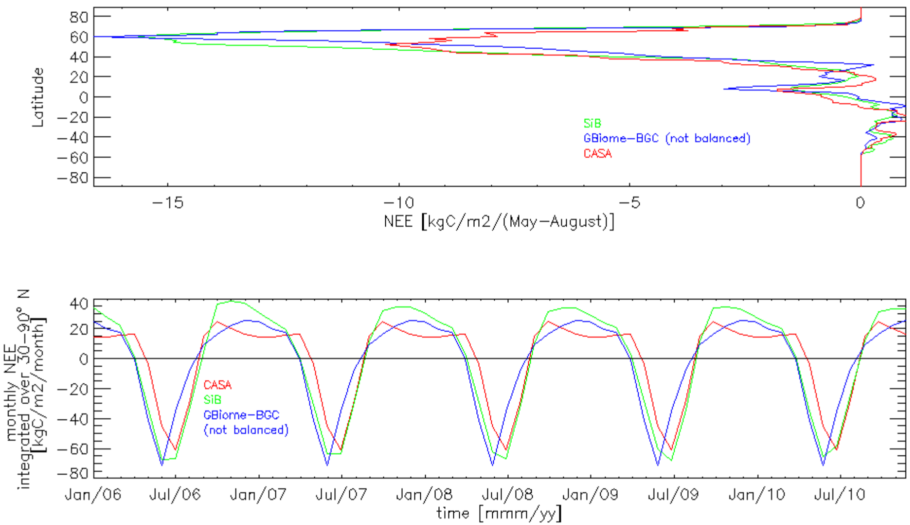

Fig. 1. Upper panel: Latitudinal NEE distributions integrated for May until August. The sink between 30° and 75° N reflects the CO_2 uptake in the boreal forest in all three models and the biggest differences between the models are found here as well. CASA has a less distinct sink than SiB and GBiome-BGC, but the large sink in the GBiome-BGC is partially due to the net yearly uptake. Bottom panel: The time series of monthly NEE integrated between 30° and 90° N. The pronounced summer sink in both, Sib and GBiome-BGC, can be seen in the seasonal cycle amplitude. The CASA amplitude is smaller and later than both SiB and GBiome-BGC. The SiB and CASA autumn releases occur simultaneously and about a month later than GBiome-BGC. This leads to the widest seasonal cycle minimum in SiB and similar widths for CASA and GBiome-BGC, shifted about a month against each other.

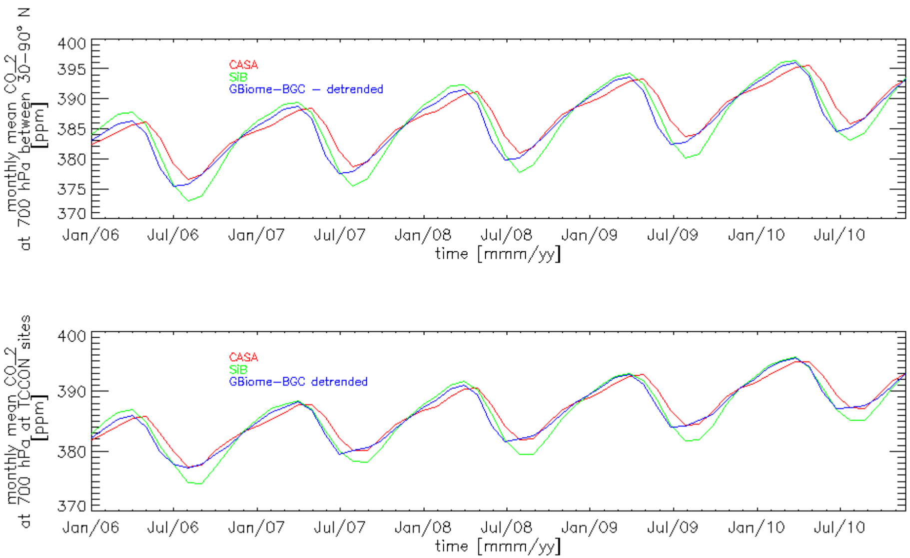

Fig. 2. Upper panel: The monthly mean CO_2 at 700 hPa between 30° and 90° N. The GEOS-Chem CO_2 simulations follow the characteristics of the NEE input model. The drawdown starts about a month earlier with the SiB and GBiome-BGC NEE estimates in contrast to the CASA estimate. The largest drawdown is found for the SiB NEE input and the smallest for the CASA NEE input. The GEOS-Chem CO_2 simulation with the GBiome-BGC was detrended for the net CO_2 uptake and has a muted amplitude compared to the GBiome-BGC NEE input. The minimum is widest for SiB and shortest for CASA. Bottom panel: the same figure, but for the monthly mean CO_2 averaged only over four TCCON sites. The important feature is that the seasonal cycles are similar to the integration over nearly the entire Northern Hemisphere.

ACPD
12, 12759–12800, 2012

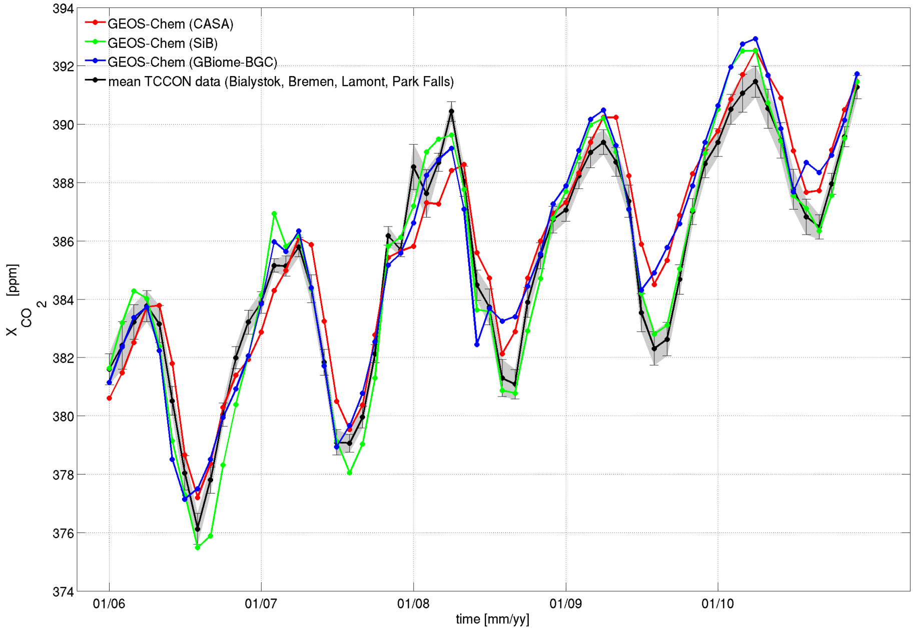

Fig. 3. The time series of the monthly averages of column averaged X_{CO_2}. The black line shows the mean for the TCCON measurements in Białystok (Poland), Bremen (Germany), Lamont (Oklahoma) and Park Falls (Wisconsin). The colored lines show the smoothed column averaged CO_2 for the three models. The same yearly pattern reveals as seen in the GEOS-Chem CO_2 simulation at 700 hPa, integrated between 30° and 90° N and averaged over the TCCON sites. In comparison with the TCCON measurements, the GEOS-Chem CO_2 simulation with the SiB NEE input seems to fit best. The variability of the TCCON timeseries in the winter of 2007–2008 is due to the few measurements averaged (Table 5).

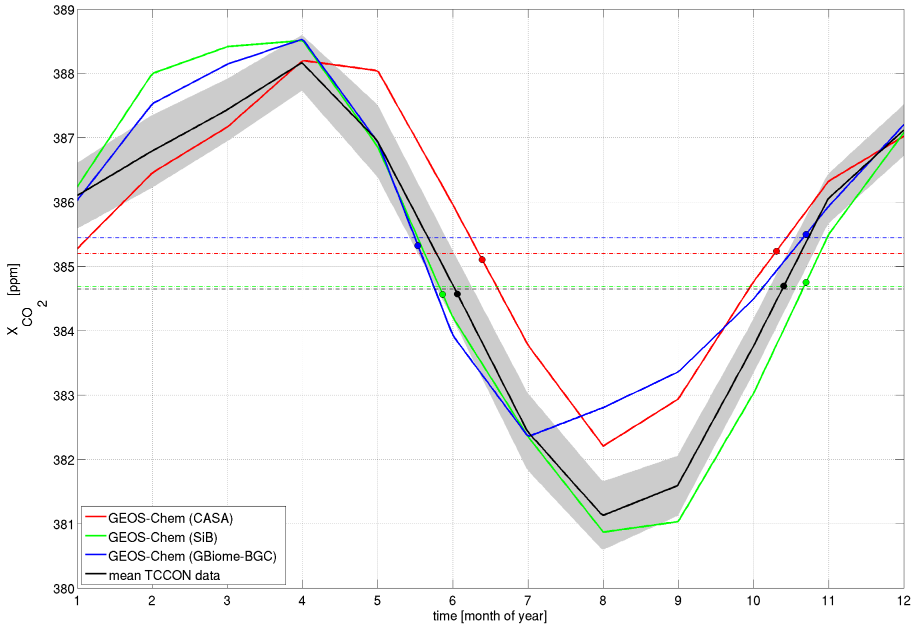

Fig. 4. Averaged seasonal cycles, derived with the averages of the monthly means, shown in Fig. 3. The emerging patterns reveal the characteristics already seen in the NEE inputs, as well as in the GEOS-Chem CO_2 simulations at 700 hPa and in the smoothed X_{CO_2}. The simulated CO_2 drawdown using SiB or GBiome-BGC starts starts too early compared to the TCCON measurements and too late using CASA inputs. The seasonal amplitude is slightly overestimated with SiB and underestimated using GBiome-BGC and CASA. The simulated CO_2 release starts too early using CASA and too late using SiB or GBiome-BGC. The crossings with the dashed lines indicate the turning points of the seasonal cycles and give an estimate of the delays in the CO_2 drawdown and release (Table 6).

ACPD
12, 12759–12800, 2012

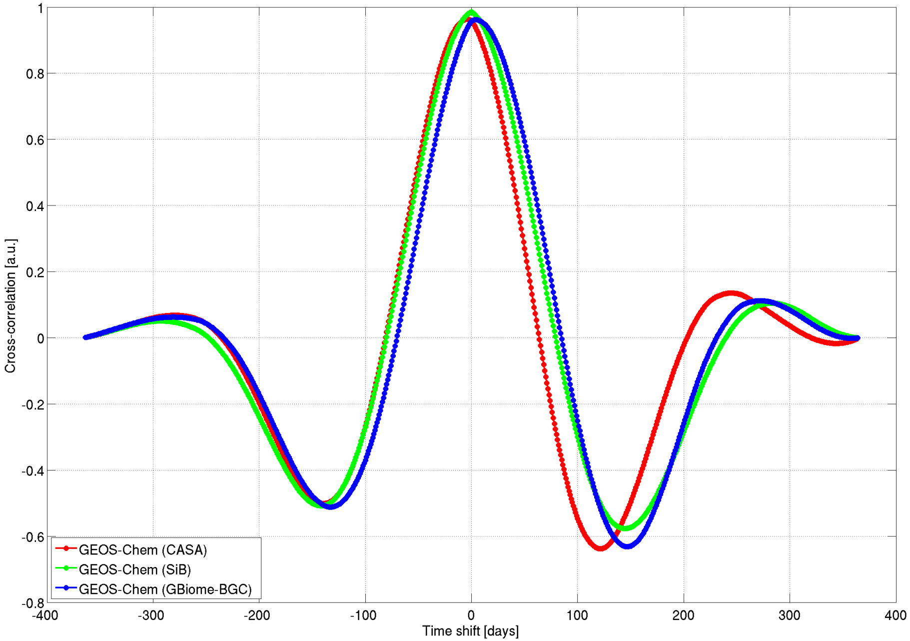

Fig. 5. The cross-correlations between the averaged seasonal cycles for the three NEE estimation models and the averaged TCCON X_{CO_2} seasonal cycle (averaged seasonal cycles shown in Fig. 4). The cross-correlation optimizes for a negative time shift for CASA and for a positive time shift for GBiome-BGC. The averaged seasonal cycle using SiB is optimized without a time shift. The time shifts in days are given in Table 6.

ACPD
12, 12759–12800, 2012

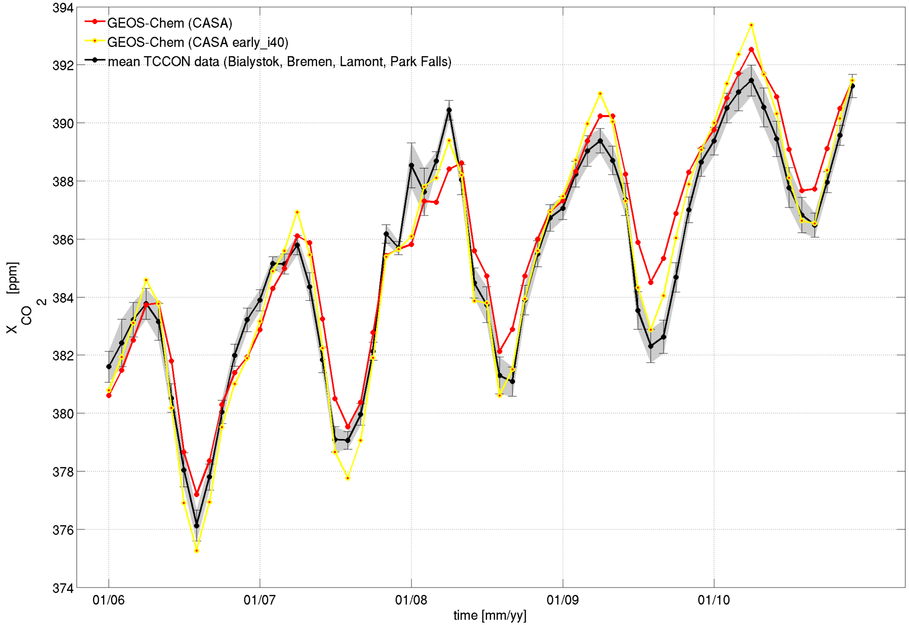

Fig. 6. The time series of the monthly averages of column averaged X_{CO_2}. The NEE was enhanced by 40 % in the boreal forest (45° N and 65° N) and the onset of the growing season shifted earlier by adding the July NEE to the May NEE between 50° N and 60° N. In comparison with the TCCON measurements, the GEOS-Chem CO_2 simulation improves significantly with these changes. The variability of the TCCON timeseries in the winter of 2007–2008 is due to the few measurements averaged (Table 5).

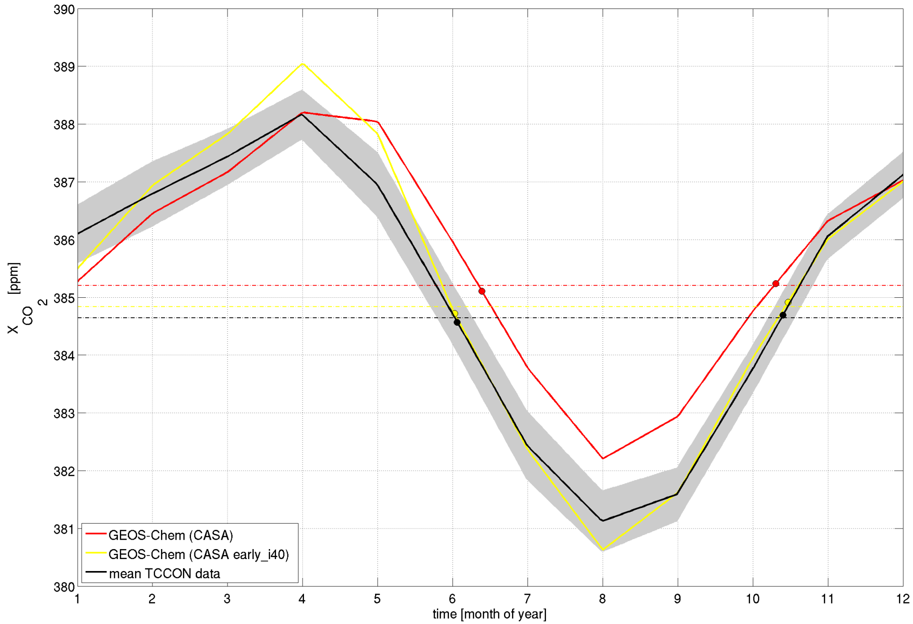

Fig. 7. Averaged seasonal cycles, derived with the averages of the monthly means, shown in Fig. 6. The enhancement of the NEE by 40 % in the boreal forest (45° N and 65° N) and the shifting of the onset of the growing season by adding the July NEE to the May NEE between 50° N and 60° N lead to a significant improvement of the simulated CO_2 cycle. Even though the seasonal amplitude is overestimated, the simulated CO_2 drawdown and CO_2 release are estimated accurately. The cross-correlation optimizes for an unchanged seasonal CO_2 cycle (Table 6).

ACPD
12, 12759–12800, 2012

Title Page
Abstract | Introduction
Conclusions | References
Tables | Figures
◀| |▶
◀ ▶
Back | Close
Full Screen / Esc
Printer-friendly Version
Interactive Discussion

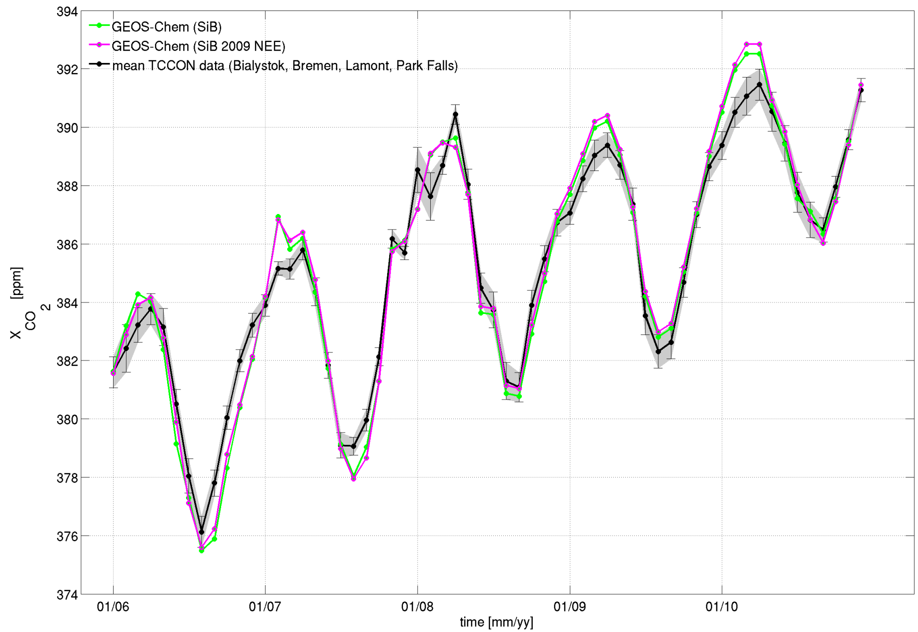

Fig. 8. The same as in Fig. 3, showing the monthly mean X_{CO_2} for the GEOS-Chem CO_2 simulation using year-specific SiB fluxes and using only SiB 2009 NEE estimations for the whole time period. The differences between these GEOS-Chem CO_2 simulations give a measure of the impact of year-specific NEE fluxes in contrast to the climatology, showing only slight differences. The variability of the TCCON timeseries in the winter of 2007–2008 is due to the few measurements averaged (Table 5).

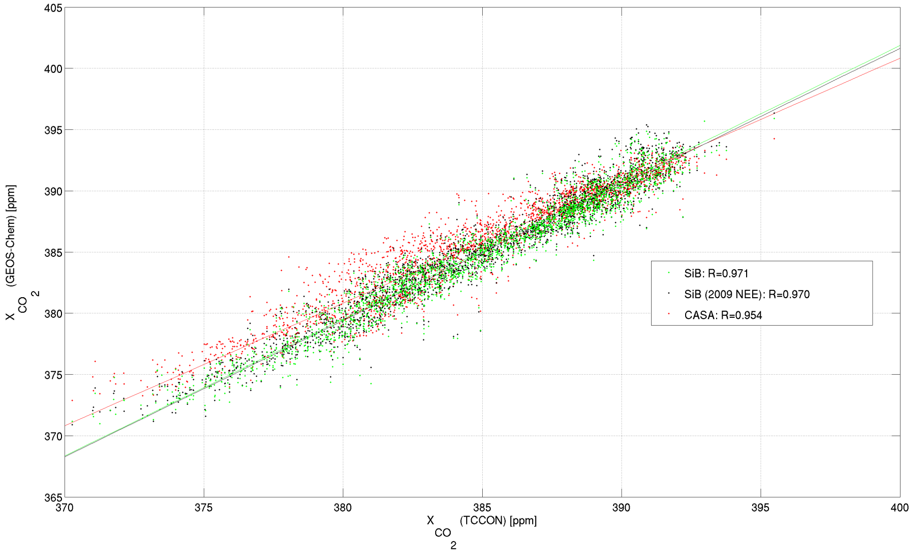

Fig. 9. Scatter plot for the GEOS-Chem CO_2 simulation using year-specific SiB fluxes (green), using only SiB 2009 NEE fluxes (black) and using CASA NEE inputs (red). The GEOS-Chem CO_2 simulation using year-specific SiB fluxes correlates best with the TCCON measurements.

ACPD
12, 12759–12800, 2012

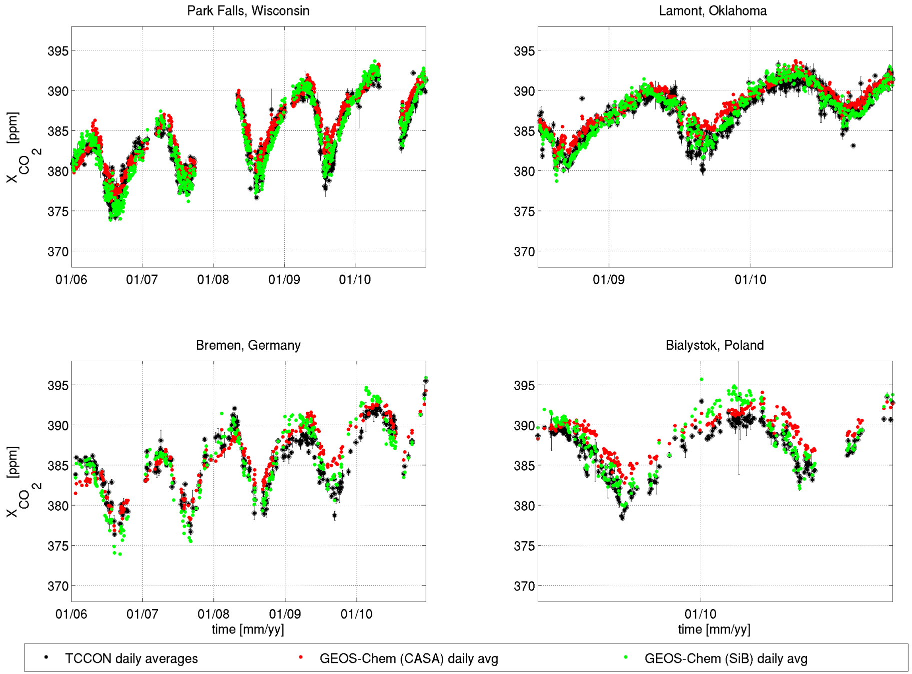

Fig. 10. GEOS-Chem CO_2 simulations using CASA NEE estimations (red dots) and SiB NEE inputs (green dots) in comparison with TCCON measurements at four sites: Park Falls (Wisconsin), Lamont (Oklahoma), Bremen (Germany), Białystok (Poland).

ACPD
12, 12759–12800, 2012

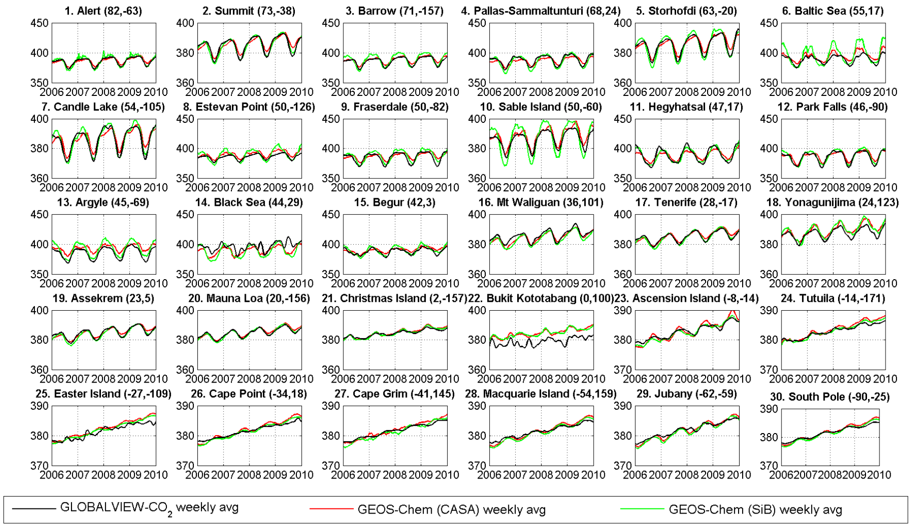

Fig. 11. GEOS-Chem CO_2 simulations using CASA NEE (red dots) and SiB NEE (green dots) in comparison with GLOBALVIEW-CO_2 data at 30 sampling locations, covering the latitude range between 82° N and 90° S.

ACPD
12, 12759–12800, 2012

Evaluation of atmosphere-biosphere exchange estimations

J. Messerschmidt et al.

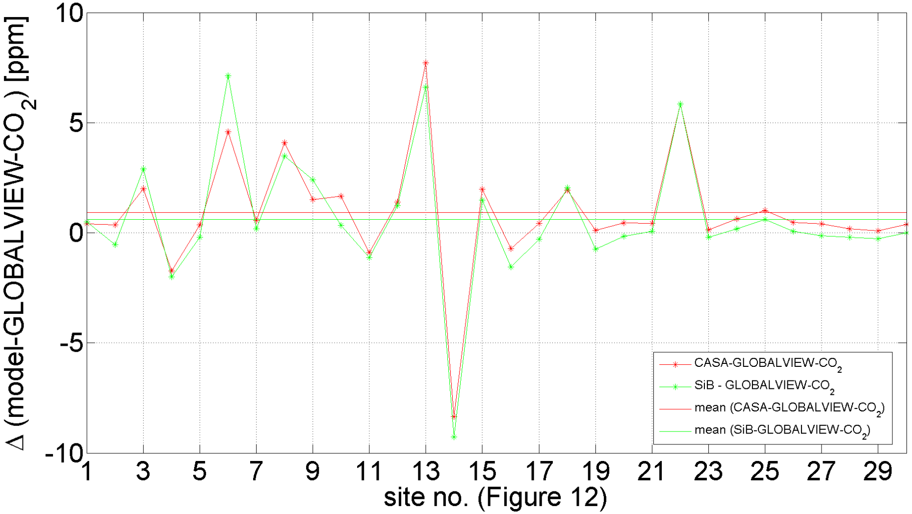

Fig. 12. Difference between GEOS-Chem CO_2 simulations using CASA NEE (red dots) and SiB NEE (green dots) with GLOBALVIEW-CO_2 data at 30 sampling locations, covering the latitude range between 82° N and 90° S.